Penerbit Akademia Baru

Journal of Advanced Research in Fluid Mechanics and Thermal Sciences

Journal homepage: www.akademiabaru.com/arfmts.html
ISSN: 2289-7879

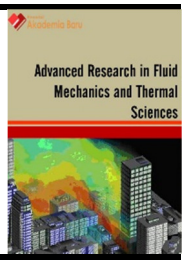

Particle Separation using Acoustic Wave Device for Microfluidic Applications

Open Access

Norazreen Abd Aziz[1,*], Mimie Asmiera Mohd Zain[1], Muhamad Ramdzan Buyong[2]

[1] Centre of Advanced Electronic and Communication Engineering (PAKET), Universiti Kebangsaan Malaysia (UKM) Selangor, Malaysia
[2] Institute of Microengineering and Nanoelectric (IMEN), Universiti Kebangsaan Malaysia (UKM) Selangor, Malaysia

ARTICLE INFO

Article history:
Received 31 August 2018
Received in revised form 30 November 2018
Accepted 2 December 2018
Available online 6 December 2018

ABSTRACT

Particle separation and sorting has become an essential step in many fields especially in medical field, biology and biochemical analysis. One of the successfully proven methods to separate the particles is through labelling process. However, this method has its limitations. One of them is that it can damage the physical properties and shorten the lifetime of the particles. Meanwhile, chip separation method by surface acoustic wave (SAW) device provides an automated and fast response process. In this separation process, standing surface acoustic waves (SSAW) induced by annular interdigitated transducer (AIDT) on piezoelectric substrate provides several distributions of pressure nodes and anti-pressure nodes in microfluidic medium. The operation frequency for AIDT is at 30.6 MHz while the RF power supply is at 20 dBM. This present study used this phenomenon to study the effects of SSAW in manipulating and separating polystyrene particles in a confined area. The separation efficiency of SAW device was analysed from various experiments conducted. A mixture of two polystyrene particles with different size suspended in deionised water was used in each experiment. The suspended particles in the liquid medium experienced acoustic radiation force within the generated SSAW. The particles with positive acoustic contras factor will move toward pressure nodes, whereas those with negative acoustic contras factor will move toward anti pressure nodes. Based on the efficiency of the separation process, it was shown that two polystyrene particles with different diameter (1 µm and 9.9 µm) have the highest separation efficiency. Thus, it can be concluded that contactless aggregation method is suitable for microfluidic applications especially in coculture cell biology, which does not affect the physical condition of cells.

Keywords:
Surface Acoustic Wave, AIDT, particle separation, microfluidic

1. Introduction

Particles separation has become one of the most important processes in various fields such as biological research, biochemical analysis, disease diagnostics and clinical practice. Recently, there are various techniques that can be used to separate the particles such as flourescene-activated cell sorting (FACS) [1], magnetic-activated cell sorting (MACS) [2], dielectrophoresis [3] and acoustic

* *Corresponding author.*
E-mail address: norazreen@ukm.edu.my (Norazreen Abd Aziz)

wave technique [4]. FACS is the first technology that has been commercialised with the ability to separate the particles. It is one of the advanced technologies that are robust and automated. Besides, FACS has the advantages of being operated in the separation process with speed of up to 50,000 cells per second [5]. However, FACS technique requires expertise in handling the equipments during the process due to the advanced technologies used. Moreover, MACS technique that used the process of labelling an external magnetic field towards the cells is also capable to isolate proteins and DNA. Although this technique has gained attention in microfluidics field, it has its own disadvantages including the ability to damage the physical properties of cells. In dielectrophoresis technique, the separation, transportation, trapping and sorting of various biological particles has been successfully demonstrated by varying the applied electric field frequency [6]. Too long exposure on electric field would induce serious joule heating effect as it will shorten the life time of particles [7] which requires integration of heat sinks mechanism [8] during the separation process.

Among these techniques, acoustic wave technology offers a great advantage due to its label-free nature procedure. Recent developments on microparticles manipulation in microfluidics using surface acoustic wave (SAW) have advanced in various ways since they use the physical properties of microparticles such as size, density and deformability for further improvement [9]. In biomedical field, the use of acoustic wave technique has been developed to separate cancer cells from red blood cells using clinical samples obtained from cancer patients [10]. The isolation of the real biological particles between white blood cells and red blood cells using acoustic wave technique has been also developed [11]. An abnormal white blood cell concentration in the human body can give serious side effect to health. In biochemical field, the separation process developed by [12] is very useful in detecting waterborne pathogens that can harm the human health through the consumption of dirty or polluted water.

Integration of surface acoustic wave separation with flow-based methods has been used to sort the particles and cells. However, the need for a sheath flow for a successful operation has become one of the main challenges. This is because the sheath flow for this method requires a complicated design. Furthermore, separation efficiency depends on the sheath liquid composition. Manipulation of the particles using bulk acoustic waves generated has been demonstrated in recent studies. However, this method is not suitable for many microfluidic devices with low acoustic reflection material including polydimethylsiloxine (PDMS) due to its high acoustic reflection coefficient.

To overcome these limitations, surface acoustic wave technique using sheathless method was investigated. This technique offers several advantages compared to other methods as it provides an automated and fast response of separation process based on size and physical properties such as density and compressibility. It also preserves the integrity, functionality and viability using label free, and contactless sorting. SAW device does not require modification of the particles in which the particles are free from external forces and do not require labelling or surface modification that can harm and shorten the life time of particles. Since its only requires a small volume of sample to be used, this separation technology can be automated and does not require expert or personnel to handle such hi-tech equipment.

Recently, concept of annular interdigitated transducer (AIDT) has been proposed to produce a strong confinement focused acoustic waves spot with of its wavelength [13]. In this work, we will for the first time experimentally demonstrate the generation of collimated acoustic waves using AIDT. We also investigate its capability when dealing with microparticles in fluidic environment. A separation method of multiple size of polystyrene particles was presented using SAW device with the objective to identify the related parameters and forces that contribute to the separation of suspended polystyrene particles in microfluidic medium. In this separation process, standing

surface acoustic wave (SSAW) induced by AIDT on piezoelectric substrate provides several distributions of pressure nodes and anti-pressure nodes in microfluidic. The suspended particles in medium experiencing acoustic radiation force are translated into pressure node and anti-pressure node. Thus, it is expected that larger particles will move toward the pressure node and the smaller particles will move toward the opposite direction.

2. Operating Principle

Conventional interdigitated transducer (IDT) structure employed in SAW has the arrangement of several electrodes connected in a coupling. Formation of IDT on the piezoelectric substrates can be realised through lithography techniques. When an alternating input signal is applied to the electrode, it forms an electric field, thus affecting the surface acoustic wave due to the impact of piezoelectric coupling. The surface acoustic will propagate away from interdigitated electrode waves acting as mechanical actuator to induce mechanical response in the environment. Modification on the electrode design from linear to annular causes the resulting surface acoustic energy to be converged at a point, which is at the centre of the device. This will result in a maximum displacement magnitude and cause the high flow of velocity to be induced.

Types of propagating waves at the centre of AIDT depend on the width of electrodes. It has been observed that surface waves will converge for electrodes of 12.5 µm width [14] while for electrodes with width of 55 µm, they will produce a standing surface waves (SSAW) propagating at the centre of the device [15]. SSAW occurs due to the primary acoustic radiation forces overlap, which induces multiple pressure nodes and anti-pressure nodes. This affects micro-particles to move toward pressure nodes or pressure-resisting nodes depending on the size, density and compression of micro-particles [16]. The primary acoustic radiation force is given by

$$F_{ac} = -\left(\frac{\pi {p_o}^2 V_c \beta_w}{2\lambda}\right) \emptyset(\beta, \rho) \sin(2kx) \tag{1}$$

$$\emptyset = \frac{5\rho_c - 2\rho_w}{2\rho_c + \rho_w} - \frac{\beta_c}{\beta_w} \tag{2}$$

Where p_o, V, β_w, β_c λ, k, x, ρ_c, ρ_w are the acoustic presure amplitude, volume of the particle, compressibility of the medium, compressibility of the particle, wavelength, wave number, distance particle from the pressure node, density of the particles and density of the medium [17]. Acoustic contrast factor is the determinant of particle movement in particle aggregation or separation process. The contras factor $(\emptyset)$ is derived from particles density and compressibility. The movements of the particles either toward the pressure nodes or anti pressure nodes are determined by the acoustic contras factor $(\emptyset)$. The particles with $(\emptyset) > 0$ will attract to the pressure nodes and the particles with $(\emptyset) < 0$ will move toward the opposite direction. The accumulation of particles at pressure nodes and anti-pressure nodes of standing wave (SSAW) by acoustic force is illustrated in Figure 1.

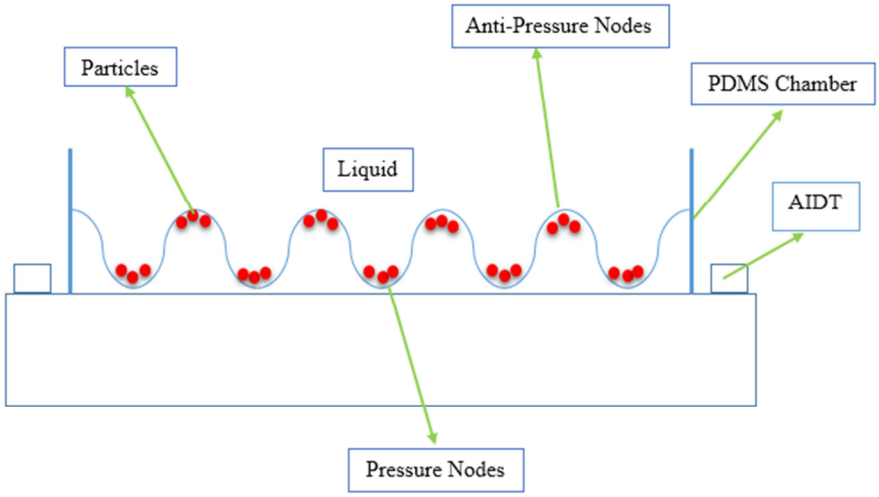

Fig. 1. Illustration of particles aggregation under the influence of acoustic radiation force

Particles are also subjected to Strokes drag force from induced acoustic streaming flow. The Strokes drag force is given by

$$F_d = 6\pi\mu ru \quad (3)$$

Where μ is the liquid viscosity, r is the radius of the particles and u is the velocity between the particles and medium. Since there was no sheath used in this experiment to control the particles toward the separation area in the device, the Strokes drag force produced was smaller compared to the acoustic radiation force. Acoustic radiation force is proportional to the third power of the particles radius while the Strokes drag force is proportional to r. This makes the migration time to move the large particles toward the standing wave to be shorter compared to that of small particles [16].

3. Experimental Setup

3.1 Fabrication Process of SAW Device

In this study, metal lift-off technique was chosen to produce an optimum annular IDT. Such technique was used to produce patterns or structures by lifting or removing photoresist layer. This was because it is considered as non-hazardous procedure and is much easier to handle any the metal thickness below 500 nm. Annular electrodes of the surface acoustic wave (SAW) device have constant width and pitch based on the floating-electrode unidirectional transducers (FEUDTs) design. FEUDT usually has more than two electrodes per wavelength. Figure 1 illustrates the fabrication steps used to develop SAW device. Starting with cleaning procedure, piezoelectric substrate was coated with HDMS layer followed by layer of photoresist AZ 5214E. Substrate was exposed to the UV using Karl Suss Mask Aligner with parameters tabulated in Table 1. Meanwhile, 20 nm thick of adhesion layer of chromium was deposited prior to metal deposition of aurum layer with 350 nm of thickness. Both thin films were deposited onto the substrate using DC sputtering method with power voltage and pressure of up to 200 W and 2 mTorr, respectively. Figure 2 shows the fabrication process flow for AIDT device. Substrate was immersed in acetone bath with low ultrasonic energy for lift process. Substrate was cut into 2 cm x 2 cm for ease of handling and was

bonded with SMA connector onto PCB for electrical measurement purpose. Figure 3 displays the SEM images of fabricated SAW device.

Table 1
Parameters for UV light exposure

Parameters	Value
Exposure time	7 s
Sample size	4“
Mask thickness	1 mm
Sample thickness	350 µm
Photoresist thickness	1 µm
Align gap	50 µm
Proximity gap	10 µm

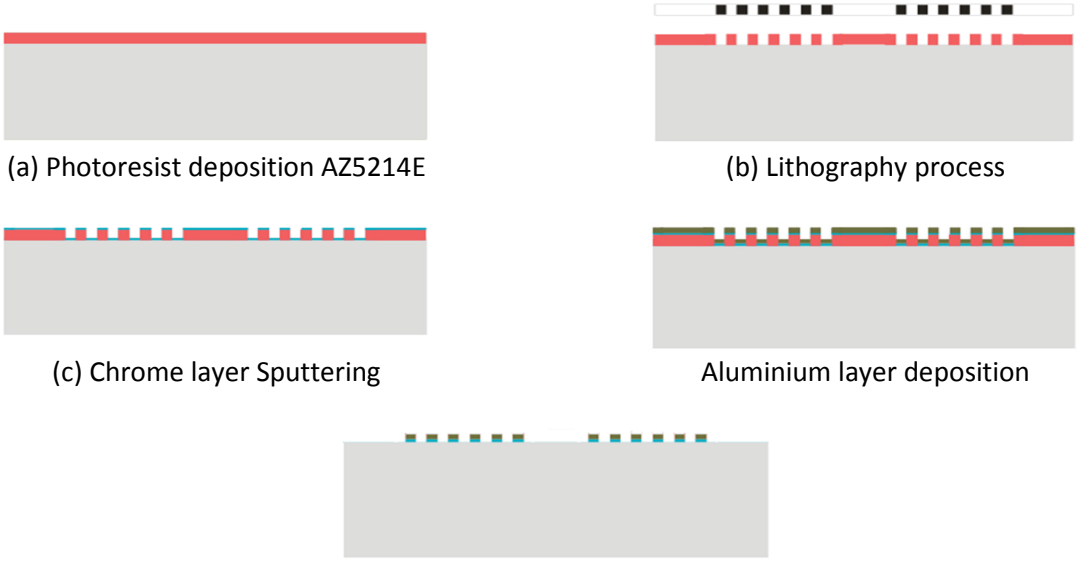

(a) Photoresist deposition AZ5214E

(b) Lithography process

(c) Chrome layer Sputtering

Aluminium layer deposition

(e) Metal lift-off

Fig. 2. Fabrication process flow for AIDT device

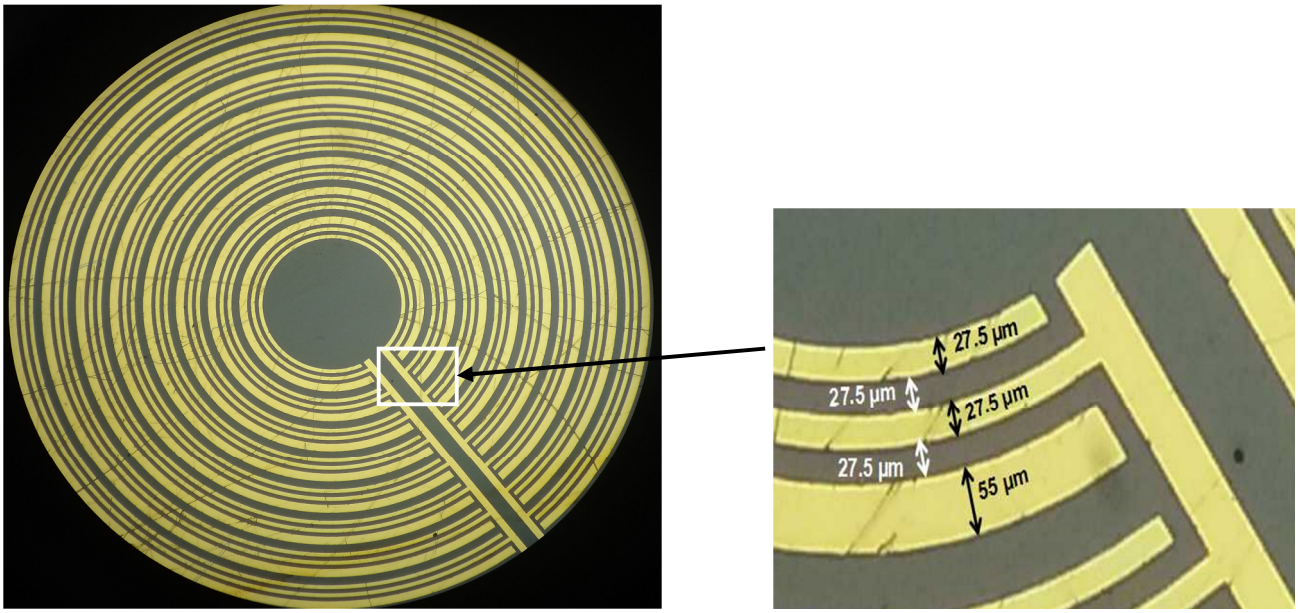

Fig. 3. (a) SEM images of fabricated SAW device (b) dimension of electrodes and gap in between them

3.2 Test Setup

Before the experiment was conducted, factors contributed to the separation of different size of particles using acoustic wave (SAW) device were identified. Parameters namely force, size of particles, density, compressibility, frequency, mixture volume, pressure amplitude and acoustic contras factor were determined and calculated as in Table 2. Suspended particles in medium were subjected to four different forces; acoustic radiation force, Stokes drag force, gravity forces and buoyant force. Gravity force and buoyant force can be ignored since both forces have the same magnitude and different direction.

Table 2
Properties of polystyrene particles

Properties of polystyrene particles	Type 1	Type 2	Type 3
Diameter (µm)	1 µm	4.8 µm	9.9 µm
Mass (%)	1	1	1
Density (g/cm^2)	0.23873× 10^{12}	2.15868× 10^9	0.24604× 10^9
Compressibility (Pa^{-1})	2.16× 10^{10}	2.16× 10^{10}	2.16× 10^{10}

Separation experiment was conducted using fabricated SAW device on a microscope (Olympus STM6). In this experiment, three different size of polystyrene particles were used; 4.8 µm 1 µm and 9.9 µm. A mixture of two different sizes of polystyrene particles suspended in deionized water with the properties as listed in Table 3 was used in each experiment with the concentration of 1:40. The mixture of each polystyrene particle injected on the device was 1 µL using a syringe pump. Device was operated by applying various levels of RF at the operating frequencies as shown in Figure 4. Meanwhile, Figure 5 shows the experimental setup of the separation process observed under high resolution microscope (Olympus STM6). Surface and bulk fluid vibrations were among the constituted mechanisms that concentrate or align particles at nodes or anti-pressure nodes along a standing wave. The accumulation of the particles either at nodes or pressure nodes were seen to depend on their size, density relative to the fluid and compressibility [2]. All the data from this experiment were recorded in a video form for analysis purposes. Snapshot images from videos were converted using MATLAB while the selected images of each experiment were analysed using imageJ software.

Table 3
Number of injected particles

Experiments	Number of injected particles (A)	Number of injected particles (B)	Frequency (MHz)
1	4.99 x 10^8 (size: 4.8 µm)	4.55 x 10^7 (size: 9.9 µm)	18
			30.6
2	4.55 x 10^{10} (size: 1 µm)	4.55 x 10^7 (size: 9.9 µm)	18
			30.6
3	4.55 x 10^{10} (size: 1 µm)	4.99 x 10^8 (size: 4.8 µm)	18
			30.6

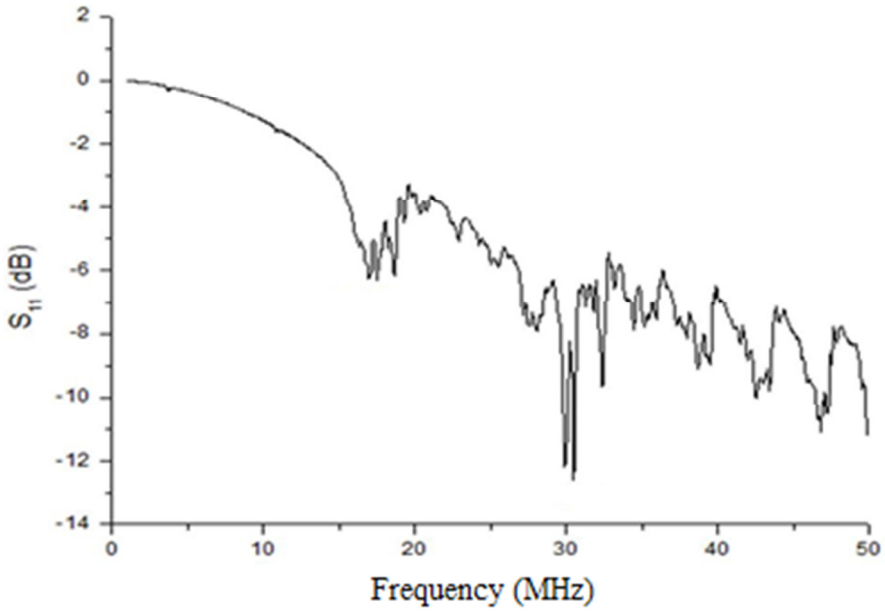

Fig. 4. Frequency response of SAW device

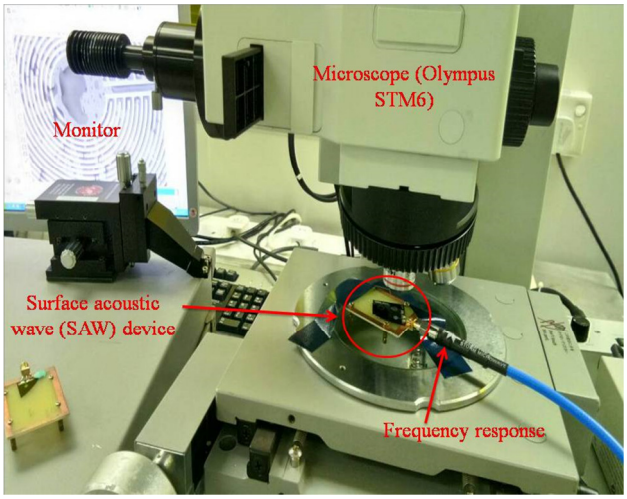

Fig. 5. Setup for the separation of suspended particles in liquid medium

4. Results and discussion

The experiment that included all three separations of a mixture of suspended particles with two different sizes under the influence of acoustic wave propagation, were recorded. During the experiment, it was observed that the device operated optimally at two dominant resonant frequencies of 18 MHz and 30.6 MHz. There are two waves that can propagate in this device, which are SAW at basic mode frequency (18 MHz) and Lamb waves at higher frequency (30.6 MHz). Each separation experiment was tested using both frequencies as shown in Table 3. For the first experiment, the movement of particles towards the pressure nodes and anti-pressure nodes had increased proportionally to the applied RF power. At operating frequency of 30.6 MHz and RF applied power of 20 dBm, separation of two different size particles was successful. Polystyrene particles of 9.9 µm in size with positive Ø-factor moved toward the pressure nodes while particles of 4.8 µm in size with negative Ø-factors moved toward anti-pressure nodes within the standing wave. As the power decreases to 15 dBM, acoustic radiation force was weakened due to less

generation of leaky wave propagation. Thus, particles aligned themselves at the every pressure nodes and anti-pressure nodes without being separated. Figure 7 depicts the successful separation procedure of 4.8 µm and 9.9 µm particles at operating frequency of 30.6 MHz with RF power applied at 20 dBM. At basic mode frequency at 18 MHz, those particles were capable to be separated at 20 dBM, but the separation process was less efficient compared to that with higher frequency and power supplied.

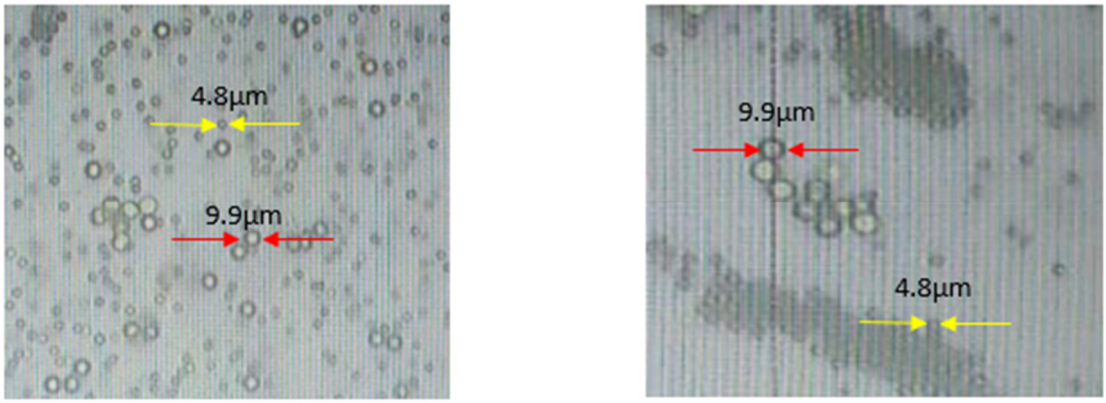

(a) (b)

Fig. 7. (a) Before and (b) after the separation process of 4.8 µm and 9.9 µm particles

This separation experiment was recorded in 2 minutes. The recorded video was converted into image clusters using MATLAB software. On average, there were 600 image sections that have been converted from each experimental video. The data obtained from each polystyrene particle separation process were selected to select the best image clusters to ensure accurate particle separation analysis. Prior to the estimation of the total number of separated particles, the image was filtered using ImageJ software. Estimation on collected particles counts in the section of pressure nodes and anti-pressure nodes was successfully recorded using the same software. Experiment 2 and 3 were conducted in a same manner as in Experiment 1. Acoustic wave propagation generated from the device induced pressure fluctuation and caused the acoustic radiation forces to form in fluidic medium enabling separation particles of size 1 µm and 9.9 µm in experiment 2 as shown in Figure 8.

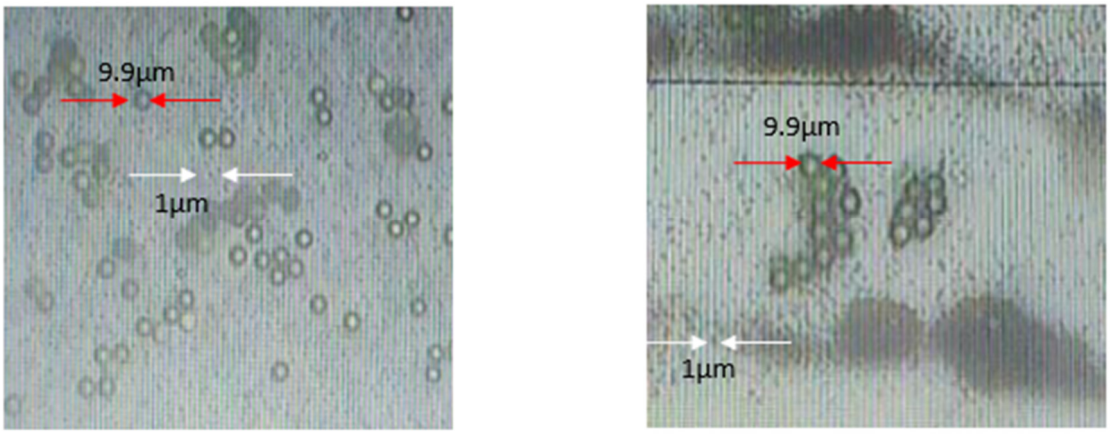

(a) (b)

Fig. 8. (a) Before and (b) after the separation process of 1 µm and 9.9 µm particles

From the figure, it was clearly observed that particles with size of 1 µm were well separated from particles of size 9.9 µm. Particles of size 9.9 µm moved and hold at anti pressure nodes due to their positive Ø-factors, whereas particles of size 1 µm moved toward anti-pressure nodes. For the last experiment involving particles of size 1 µm and 4.8 µm, it was seen that both particles were positioned and aligned at anti-pressure nodes of the standing wave generated. This was due to their similar negative Ø-factors as shown in Figure 9. The sign of the Ø-factors calculated and the position of various particles used in this experiment are shown in Table 4.

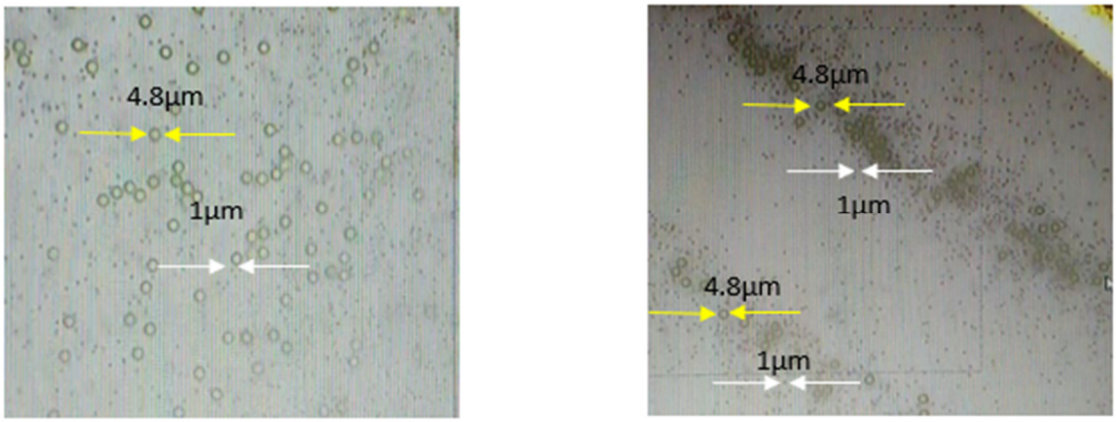

(a) (b)

Fig. 9. (a) Before and (b) after the separation process of 1 µm and 4.8 µm particles

Table 4
Particle parameters during separation experiment

Size of particles [µm]	Ø-factors	Movement of the particles
1 µm	Negative	Anti-node
4.8 µm	Negative	Anti-node
9.9 µm	Positive	Pressure node

Each liquid sample was smeared on the device using rectangular glass slide to ensure that the liquid medium is in fully contact with the generated acoustic radiation force. Large volume of liquid resulting higher Strokes drag force in the medium and the acoustic radiation force was diminished. During the experiment, it was observed that there were small amounts of polystyrene particles that were not trapped at the nodes. This was due to the Strokes drag force, which were significant in the areas with a weak acoustic wave radiation, which were at both end of the SSAW. Separation efficiency of SAW device in separation two different sizes particles was analysed from these three experiments. The separation efficiency can be expressed as

$$\text{Efficiency, \%} = \frac{n_{collected}}{n_{injected}} \times 100\% \quad (4)$$

Where $n_{\text{collected}}$ is the average number of particles trapped in the separation area and n_{injected} is the average number of total polysterene particles injected at the beginning of experiment. Table 5 shows the separation efficiency of the polystyrene particles of the three experiments conducted. Tabulated data in the table shows that Experiment 2 (1 µm and 9.9 µm) produced highest separation efficiency of 88.3% followed by Experiment 1 with 81.8%. On average, 79.1% of particles (1 and 4.8) were aggregated in each anti-pressure node generated within the device. Based on these findings, in can be concluded that this method is suitable for lower selectivity particles separation. Higher selectivity separation could be achieved at higher RF power.

Table 5
Separation efficiency of polystyrene particles

Experiment	Separation efficiency (%)
1	81.8
2	88.3
3	79.1

5. Conclusions

In summary, the separation process of two suspended particles that are different in size in liquid medium has been successfully implemented. Particles with different size have been sorted and located in the confined area of SAW device. It can be concluded that selectivity of particles separation is affected by the RF power applied. The efficacy of the separation process was based on the size of particles, RF input power applied, acoustic radiation forces and liquid volume. This on chip separation method by SAW device has provided an automated and fast response process.

Acknowledgement
Authors would like to gratefully acknowledge this work, which was financially supported by the Universiti Kebangsaan Malaysia (UKM) and Ministry of Education of Malaysia through a grant project (code no: GGPM-2017-035).

References
[1] Applegate, Robert W., Jeff Squier, Tor Vestad, John Oakey, and David WM Marr. "Optical trapping, manipulation, and sorting of cells and colloids in microfluidic systems with diode laser bars." *Optics express* 12, no. 19 (2004): 4390-4398.
[2] Xia, Nan, Tom P. Hunt, Brian T. Mayers, Eben Alsberg, George M. Whitesides, Robert M. Westervelt, and Donald E. Ingber. "Combined microfluidic-micromagnetic separation of living cells in continuous flow." *Biomedical microdevices* 8, no. 4 (2006): 299.
[3] Diaz, R., and S. Payen. "Biological cell separation using dielectrophoresis in a microfluidic device." *Bio and Thermal Engineering Laboratory–University of California B (ed). http://robotics. eecs. berkeley. edu/% 7Epister/245/project/DiazPayen. pdf* (2008).
[4] Dauson, E. R., K. B. Gregory, I. J. Oppenheim, G. P. Healy, and D. W. Greve. "Particle separation using bulk acoustic waves in a tilted angle microfluidic channel." In *Ultrasonics Symposium (IUS), 2015 IEEE International*, pp. 1-4. IEEE, 2015.
[5] Herzenberg, Leonard A., David Parks, Bita Sahaf, Omar Perez, Mario Roederer, and Leonore A. Herzenberg. "The history and future of the fluorescence activated cell sorter and flow cytometry: a view from Stanford." *Clinical chemistry* 48, no. 10 (2002): 1819-1827.
[6] Buyong, Muhamad Ramdzan, Jumril Yunas, Azrul Azlan Hamzah, B. Yeop Majlis, F. Larki, and N. Abd Aziz. "Design, fabrication and characterization of dielectrophoretic microelectrode array for particle capture." *Microelectronics International* 32, no. 2 (2015): 96-102.
[7] Qian, Cheng, Haibo Huang, Liguo Chen, Xiangpeng Li, Zunbiao Ge, Tao Chen, Zhan Yang, and Lining Sun. "Dielectrophoresis for bioparticle manipulation." *International journal of molecular sciences* 15, no. 10 (2014): 18281-18309.
[8] Razali, A. A., and A. Sadikin. "CFD simulation study on pressure drop and velocity across single flow microchannel heat sink." *J. Adv. Res. Des.* 8 (2015): 12-21.
[9] Gossett, Daniel R., Westbrook M. Weaver, Albert J. Mach, Soojung Claire Hur, Henry Tat Kwong Tse, Wonhee Lee, Hamed Amini, and Dino Di Carlo. "Label-free cell separation and sorting in microfluidic systems." *Analytical and bioanalytical chemistry* 397, no. 8 (2010): 3249-3267.
[10] Li, Peng, Zhangming Mao, Zhangli Peng, Lanlan Zhou, Yuchao Chen, Po-Hsun Huang, Cristina I. Truica *et al.,* "Acoustic separation of circulating tumor cells." *Proceedings of the National Academy of Sciences* 112, no. 16 (2015): 4970-4975.
[11] Ding, Xiaoyun, Zhangli Peng, Sz-Chin Steven Lin, Michela Geri, Sixing Li, Peng Li, Yuchao Chen, Ming Dao, Subra Suresh, and Tony Jun Huang. "Cell separation using tilted-angle standing surface acoustic waves." *Proceedings of*

the National Academy of Sciences 111, no. 36 (2014): 12992-12997.
[12] Jimenez, Melanie, Brian Miller, and Helen L. Bridle. "Efficient separation of small microparticles at high flowrates using spiral channels: application to waterborne pathogens." *Chemical Engineering Science* 157 (2017): 247-254.
[13] Laude, Vincent, Davy Gérard, Naima Khelfaoui, Carlos F. Jerez-Hanckes, Sarah Benchabane, and Abdelkrim Khelif. "Annular interdigital transducer focuses piezoelectric surface waves to a single point." *arXiv preprint arXiv:0712.3899*(2007).
[14] Laude, Vincent, Kimmo Kokkonen, and Sarah Benchabane. "Characterization of surface acoustic wave focusing by an annular interdigital transducer." In *Ultrasonics Symposium (IUS), 2009 IEEE International*, pp. 919-922. IEEE, 2009.
[15] Norazreen Abd Aziz, PhD Thesis 2017. *Optimization of Surface Acoustic Wave Focusing by AIDT for Microfluidcs Application*. Universiti Kebangsaan Malaysia.
[16] Soliman, A., M. Eldosoky, and T. Taha. "Modelling and simulation of microparticles separation using standing surface acoustic waves (SSAWs) microfluidic devices for biomedical applications." *Int. J. Comput. Appl* 129 (2015): 30-38.
[17] Muller, Peter Barkholt, Rune Barnkob, Mads Jakob Herring Jensen, and Henrik Bruus. "A numerical study of microparticle acoustophoresis driven by acoustic radiation forces and streaming-induced drag forces." *Lab on a Chip* 12, no. 22 (2012): 4617-4627.